



HAL
open science

Starting the winter season: predicting endodormancy induction through multi-process modeling

Guillaume Charrier

► **To cite this version:**

Guillaume Charrier. Starting the winter season: predicting endodormancy induction through multi-process modeling. 2021. hal-03065757v2

HAL Id: hal-03065757

<https://hal.inrae.fr/hal-03065757v2>

Preprint submitted on 31 Mar 2021 (v2), last revised 24 Nov 2021 (v3)

HAL is a multi-disciplinary open access archive for the deposit and dissemination of scientific research documents, whether they are published or not. The documents may come from teaching and research institutions in France or abroad, or from public or private research centers.

L'archive ouverte pluridisciplinaire **HAL**, est destinée au dépôt et à la diffusion de documents scientifiques de niveau recherche, publiés ou non, émanant des établissements d'enseignement et de recherche français ou étrangers, des laboratoires publics ou privés.

1 **Starting the winter season: predicting endodormancy induction in walnut**
2 **trees through multi-process modeling.**

3

4 **Running title: Predicting endodormancy induction in walnut trees**

5

6 Guillaume Charrier¹

7 ¹Université Clermont Auvergne, INRAE, PIAF, 63000 Clermont-Ferrand, France

8 *: corresponding author

9 Email: guillaume.charrier@inrae.fr

10 Tel: +33 4 43 76 14 21

11 UMR PIAF, INRAE Site de Crouel

12 5, chemin de Beaulieu

13 63000 Clermont-Ferrand

14

1 **Abstract**

2 *Background and Aims*

3 In perennial plants, the annual phenological cycle is sub-divided into successive stages whose
4 completion will lead directly to the onset of the following event. A critical point is the transition
5 between the apparent vegetative growth and the cryptic dormancy. To date, the initial date for
6 chilling accumulation (D_{CA}) is arbitrarily set using various rules such as fixed or dynamic dates
7 depending on environmental variables. These rules led to tremendous variability across studies
8 and sites (from late summer until late autumn).

9 *Methods*

10 To test the relevancy of different D_{CA} , a dataset combining 34 dormancy release dates and 77
11 budburst dates in independent locations and/or years and 111 frost hardiness measurements in
12 various orchards across France and Spain for the walnut *Juglans regia* L. cv Franquette.

13 *Key Results*

14 Many of the tested D_{CA} provided accurate results for the calibration and validation datasets
15 ($RMSEP < 10$ and 8 days for endodormancy release and budburst dates, respectively).
16 However, for frost hardiness, only the D_{CA} provided by the DORMPHOT model provided
17 accurate results ($RMSEP < 3^{\circ}C$). The best D_{CA} was thus selected using a composite index for
18 all three processes.

19 Testing the prediction under current and future climatic scenario showed that in, up to 25% of
20 French territory under RCP 8.5 scenario, ecodormancy stage is likely to be delayed although
21 temperature is increasing. Overall, less average frost damages are expected although decennial
22 risk (*i.e.* return period of ten years) is likely to increase in autumn in 15% of French territory.

23 *Conclusions*

1 In southern part of France, delayed dormancy induction and release would induce delayed
2 budburst and blooming altering flower and fruit production, whereas North East and Massif
3 Central parts of France may suffer higher frost risks from late frost acclimation. Finally, this
4 study describes relationships between climatic variables and plant phenological processes to
5 build metamodels predicting next century's phenological cycles at the global scale.

6

7 **Keywords:** Chilling, Frost acclimation, Frost damages, *Juglans regia* L, Photoperiod,
8 Phenology, Projection, Risk assessment, Trees.

1 **Introduction**

2 In frost-exposed environments, deciduous trees have to timely adjust their biology and
3 increase frost resistance by anticipating unfavorable conditions before the winter period. As
4 observed for most stresses, avoidance and tolerance are two complementary processes driving
5 frost resistance (Charrier *et al.*, 2011). The protection of shoot apical meristems under bud
6 scales can be considered as an avoidance strategy. This is achieved through physiological
7 changes allowing the transition from an apparently active (*e.g.* primary and secondary growth,
8 leaf expansion, fruit maturation) towards a ‘dormant’ period. In temperate species, dormancy
9 is a two-stage period with respect to the inhibiting factor. During endodormancy (formerly
10 called dormancy), growth is inhibited by intrinsic factors to the bud (‘endo’) whereas during
11 ecodormancy (formerly called quiescence), growth is limited by environmental factors (‘eco’;
12 Lang *et al.*, 1987). During this transition, different phenologically-related processes that are
13 either visible (*e.g.* growth cessation, leaf fall, lignification or budset) or invisible (*e.g.* dormancy
14 induction and release) take place. In parallel, trees transiently increase their frost tolerance
15 through frost acclimation / deacclimation process (Charrier *et al.*, 2011).

16 In autumn, endodormancy release and frost acclimation are induced by the same
17 environmental factors, namely decreasing temperature and photoperiod (Welling *et al.*, 2002;
18 Arora *et al.*, 2003; Maurya & Bahlerao, 2017). After endodormancy was released, ecodormancy
19 and frost deacclimation also occurs in parallel, under the control of warm temperature, in most
20 species, eventually modulated by photoperiod in photosensitive species, such as late
21 successional species (Basler & Körner, 2012). Process-based models using these variables as
22 input have been developed to simulate the dormancy release and budburst dates (Chuine *et al.*,
23 2016), as well as frost hardiness (*e.g.* Leinonen 1996; Ferguson *et al.*, 2011; Charrier *et al.*,
24 2018).

1 Under the context of global change, it is particularly critical to accurately predict future
2 trends in warmer climates. Since the first empirical model describing the relation between
3 temperature and plant development, through the thermal-time concept (Réaumur, 1735),
4 budburst and blooming models were only computing accumulation of growth-effective
5 temperature (*i.e.* growth degree days GDD). As the starting point was set at the coldest period
6 of the year (*i.e.* January 1st or July 1st in northern and southern hemisphere, respectively), these
7 models provided accurate results. However, this type of model was not efficient under warmer
8 winter areas, where temperate crop species were attempted to grow (*e.g.* Northern Africa,
9 Middle East or South America; Balandier *et al.*, 1993). In this context, temperate perennial
10 crops did exhibit lack of chilling and insufficient endodormancy release (Weinberger, 1950).
11 The process of endodormancy, and related chilling accumulation, had thus been introduced into
12 models (Weinberger, 1956; Vegis 1964). In the recent decades, naturally growing trees have
13 also been affected by a reduction in chilling exposure throughout winter, enhancing the interest
14 into the endodormancy stage (Gauzere *et al.*, 2019).

15 Two-step models, simulating endo- and ecodormancy stages, are now commonly used to
16 predict budburst dates (Chuine *et al.*, 2016). Frost acclimation models use similar formalism
17 with direct linkage between frost acclimation and exposure to chilling temperatures followed
18 by frost deacclimation and exposure to forcing temperatures, respectively. In perennial plants,
19 the completion of a stage is concomitant with the onset of the following one (Hänninen &
20 Tanino, 2011). However, the initial date for chilling accumulation (D_{CA}) is usually arbitrarily
21 set with various rules leading to tremendous variability across studies (from late summer until
22 late autumn). Four different concepts of D_{CA} have been used (see Tab. S1):

23 - Fixed date across years and locations: from September 1st (Chuine *et al.*, 2016) until
24 November 1st (Weinberger, 1967), for northern hemisphere,

- 1 - Dynamic date through a simple climatic threshold: critical temperature (*e.g.* date of the first
2 frost; Landsberg, 1974) or photoperiod (Welling *et al.*, 1997),
- 3 - Dynamic date through a mathematic function using a single variable such as the date of
4 minimum chilling units computed by the Utah model (Richardson *et al.*, 1974),
- 5 - Dynamic date through a mathematic function using interacting variables (temperature and
6 photoperiod) simulating leaf fall date (Delpierre *et al.*, 2009) or dormancy induction
7 (DORMPHOT; Caffarra *et al.*, 2011a).

8 These different approaches have mainly been used for phenological cycle prediction. Thanks
9 to a large dataset combining data from 50 years in various orchards across France and Spain for
10 *J. regia* cv Franquette, different formalism were tested to compute the effects of the onset of
11 chilling accumulation D_{CA} on the accuracy of three related processes (endodormancy,
12 ecodormancy and frost acclimation/deacclimation). The optimal model was subsequently
13 assessed for future climate prediction over France following three contrasted *scenarii*.

14 **Material and methods**

15 *Endodormancy release and budburst dates*

16 Endodormancy release dates were measured using the one-node-cutting ‘forcing’ test of
17 Rageau (1982). Samplings were performed every three weeks from October until May and 48
18 one-node cuttings prepared per sampling date. Buds were isolated from other parts of plant to
19 prevent correlative inhibitions (Dennis, 2003). At each sampling date, one-year-old stems were
20 sampled from five individual trees and cut in 7-cm long pieces, bearing only one node at the
21 top or less than 1 cm below the top end, for terminal and axillary buds, respectively. For axillary
22 buds, the top of the cutting was covered by paraffin wax to prevent desiccation. The bases of
23 the cuttings were immersed into tap water, weekly changed. Forty-eight cuttings were exposed
24 to optimal conditions for growth resumption (*i.e.* 16/8 hours Day/Night and 25°C constant) and

1 individually observed every 3 days. Mean time until budburst (stage 09 BBCH; Meier, 2001)
2 were computed from individual time until budburst for each cutting. After endodormancy
3 release, buds of *J. regia* cv Franquette break out after 20 days under optimal conditions
4 (Mauget, 1980; Charrier *et al.*, 2011). Endodormancy release dates were thus obtained by linear
5 interpolation between the two dates giving a time to budburst higher (or equal to) and lower (or
6 equal to) than 20 days, respectively. Budburst in the field was monitored every two to three
7 days at the different sites on five individual trees until 50% of buds reached the stage 09 of the
8 BBCH scale. The different locations and number of yearly observation are indicated in Table
9 1.

10 *Frost hardiness*

11 Frost hardiness was measured from September until budburst on five one-year-old branches
12 from different individual trees in different orchards (Tab. 1) using the electrolyte leakage
13 method (Charrier & Améglio 2011). Samples were cut into six 7-cm-long segments without
14 buds. Four of them were exposed for one hour to four different freezing temperatures among
15 this set of temperatures: -5, -10, -15, -20, -30 and -40 °C. Depending on the season, either the
16 highest or the lowest temperatures were not used. Two supplementary subsamples were
17 exposed to control (+5 °C) and maximal freezing temperature (-80 °C). Freezing and thawing
18 rates were set to 5 K h⁻¹.

19 Relative electrolytic leakage (REL) was calculated as (C1/C2) as described in Zhang &
20 Willison (1987). A sigmoidal relationship between REL and temperature (θ) was assumed for
21 each sample:

$$22 \quad REL = \frac{a}{1+e^{b(c-\theta)}} + d \quad (1)$$

23 where parameters a and d define asymptotes of the function, and b is the slope at the inflection
24 point c.

1 Frost hardiness was defined as the temperature of the inflection point (c) of the adjusted logistic
2 sigmoid function (Repo & Lappi 1989), whereas frost sensitivity was considered to be estimated
3 by the parameter b in percent damage per Celsius degree. The different locations and number
4 of years and sampling dates are indicated in Table 1.

5 *Climate data*

6 Models were fit using observed daily mean and minimal temperature monitored by weather
7 station, located most of the time in the same orchard and closer than 10km distance (Tab. 1).
8 For predictive purpose, the temperature, calculated according to the CNRM-ALADIN52 model
9 and corrected by a Q-Q method (Déqué *et al.*, 2007), were used from 8462 sites across France
10 (Safran grid at 64km² spatial resolution; MétéoFrance). Four datasets were used as input
11 variable: reference period (1950-2005) and three contrasted climatic *scenarii* (RCP 2.6, RCP
12 4.5 and RCP 8.5) for the future period (2005-2100). For each site and day, day and night length
13 were computed depending on the latitude and day of year.

14 *Endodormancy induction and onset of chilling accumulation*

15 Date of the onset of chilling accumulation (D_{CA}) was computed through different functions:

- 16 i) Fixed D_{CA} every *ca.* 10 days from DOY 182 (July 1st) until DOY 335 (November 30th).
- 17 ii) Dynamic D_{CA} based on threshold values reached by minimum temperature (T_{min}), mean
18 temperature (T_{mean}), first frost (FF) or photoperiod.
- 19 iii) Date of minimum chilling units (CU_{min}) were computed according to the Utah model
20 (originally developed on *Prunus persica* L. Batsch) that computes negative chilling effect
21 for temperature higher than 16°C (Richardson *et al.*, 1974). Daily CU started were summed
22 from DOY 182 (July 1st) until DOY 365 (December 31st) using the Utah_Model function
23 (ChillR package; Luedeling, 2019).

- 1 iv) Predicted leaf fall dates (BBCH 97) were computed according to the thermal (LFT) and
2 photothermal (LFPT) models developed by Delpierre *et al.* (2009) and developed in
3 *Quercus* and *Quercus + Fagus*, respectively. Below a critical photoperiod, temperature
4 colder than a threshold, modulated by a photoperiod function in the case of the LFPT
5 model, are summed up to a critical value (Y_{crit}), corresponding to the leaf fall date. Both
6 LFT and LFPT model were computed using the original or a modified set of parameters:
7 $LF(P)T_{ori}$ and $LF(P)T_{mod}$, respectively.
- 8 v) The dormancy induction state (DS) was computed according to the DORMPHOT model
9 developed in *Betula pubescens* Ehrh. by Caffarra *et al.* (2011a). The two sigmoidal response
10 function to low temperature and photoperiod, respectively interact through sigmoidal
11 functions. The original (DP_{ori}) and two modified (DP_E and DP_L , for early and late,
12 respectively) sets of parameters were used.

13 *Endodormancy release and budburst*

14 Starting from D_{CA} , the sum of CU was modeled according to the inverse of the Richardson
15 function (Richardson *et al.*, 1974) which was defined as the best function predicting
16 endodormancy release dates in walnut trees (Chuine *et al.*, 2016; Charrier *et al.*, 2018).
17 According to the sequential paradigm, the date where $CU(t)$ reaches the critical threshold CU_{crit}
18 (arbitrary chilling units, CU) is the date of endodormancy release (D_{ER}), or the transition
19 between endodormancy and ecodormancy!

$$20 \quad CU(t + 1) = CU(t) + Max(Min(T_{high} - \theta(t); T_{high} - T_{low}); 0) \quad (2)$$

21 with $CU(t)$, the chilling unit at day t , T_{high} , both the temperature above which CU equals 0 and
22 the amount of CU when temperature equals T_{low} or lower; CU being linear between T_{low} and
23 T_{high} .

1 The ontogenetic development during ecodormancy stage was modeled according to a
 2 sigmoid function (Caffarra *et al.*, 2011a). The date when $FU(t)$ reaches the critical threshold
 3 FU_{crit} (arbitrary forcing units, FU) is the budburst date (D_{BB}).

$$4 \quad FU(t + 1) = FU(t) + \frac{1}{1 + e^{-slp(\theta(t) - T_{50})}} \quad (3)$$

5 with $FU(t)$, the forcing unit at day t , slp , the slope of the function at the temperature inducing
 6 half of the maximal apparent growth rate T_{50} .

7 *Frost hardiness and frost damages*

8 Frost hardiness and subsequent frost damages were computed using a photothermal model
 9 developed on *Pinus sylvestris* L. (Leinonen, 1996) and adapted on *Juglans regia* (Charrier *et*
 10 *al.*, 2018). Shortly, hardening ability (C_R) changes in relation to the different stage of the annual
 11 cycle (endodormancy induction, endodormancy release, ecodormancy and growth). During
 12 endodormancy and growth stages, C_R was set to 1 and 0, respectively. During endodormancy
 13 induction, C_R was either considered gradually increasing from 0 to 1 during the 30 days before
 14 the onset of chilling accumulation (Fixed D_{CA}). For simple dynamic D_{CA} , C_R was set to 0 until
 15 the threshold was reached (CU_{min} , FF , T_{min} , T_{mean} or Photoperiod). For models describing
 16 continuous process, C_R was defined as the ratio between the related variable and its critical
 17 threshold (LF, LFPT and DP models). From the interaction between hardening, temperature
 18 and photoperiod, a dynamic potential state of hardiness is computed throughout the year. Daily
 19 changes in actual frost hardiness (FH) tend to reduce the difference between potential state of
 20 hardiness and FH with a temporal lag (see complete description of the model in the original
 21 publication). Frost damages are computed on a daily basis through the relation between FH,
 22 frost sensitivity (FS, slope at FH) and minimum temperature θ_{min} as:

$$23 \quad FD = \frac{1}{1 + e^{FS(FH - \theta_{min})}} \quad (4)$$

24 *Model calibration depending on the onset of chilling accumulation*

1 Three different sub-models, namely endodormancy release, ecodormancy release and frost
2 hardiness, were calibrated one after the other, as they were interrelated. To minimize sums of
3 square between observed and predicted values, the nls function was used (Gauss-Newton
4 algorithm), with different sets of starting values at minimum, average and maximum ranges of
5 parameter realistic values.

6 For endodormancy release model, one parameter was optimized (Tab. S2): CU_{crit}
7 corresponding to the sum of chilling units to release endodormancy. The other parameters were
8 set to the values defined by Chuine *et al.* (2016). The dataset was split into calibration and
9 validation datasets containing 18 observations from 6 sites and 16 observations from 5 sites,
10 respectively (Tab. 1).

11 For ecodormancy model, one parameter was optimized (Tab. S2): FU_{crit} corresponding to
12 the sum of forcing units to break buds. The endodormancy model used to predict D_{ER} was the
13 best from the previous step and the other parameters set to the values described in Charrier *et*
14 *al.* (2018). The dataset was split into calibration and validation datasets containing 41
15 observations from 7 sites and 36 observations from 4 sites, respectively (Tab. 1).

16 For frost hardiness model, seven parameters were optimized (Tab. S2): T_1 (Upper limit of
17 the efficient temperature range), T_2 (Lower limit of the efficient temperature range), NL_1
18 (Lower limit of the efficient nyctiperiod range), NL_2 (Upper limit of the efficient nyctiperiod
19 range), δ (Part of FH_{Max} under temperature control), τ (Time constant) and FU_{critR} (Amount of
20 forcing units for hardening competence). The endodormancy and ecodormancy models used to
21 predict D_{ER} and D_{BB} , were the best from the previous steps and the other parameters set to the
22 values described in Charrier *et al.* (2018). The dataset was split into calibration and validation
23 datasets containing 60 observations (6 winter periods) from 2 sites and 51 observations (5
24 winter periods) from 5 sites, respectively (Tab. 1).

1 The quality of the fit and the predictive ability of the models depending on D_{CA} were assessed
 2 for calibration and validation datasets computing Root Mean Square Error (RMSE) and
 3 Predictive Root Mean Square Error (RMSEP), respectively:

$$4 \quad RMSE(P) = \sqrt{\frac{\sum_{i=1}^n (\hat{y}_i - y_i)^2}{n}} \quad (5)$$

5 with \hat{y}_i the predicted values for an observation I and y_i the observed values for an observation i

6 As the different D_{CA} provided contrasted results among models, a composite performance index
 7 was used, defined as :

$$8 \quad PI = \frac{RMSE_{endoD_i}}{\max(RMSE_{endoD})} + \frac{RMSE_{ecoD_i}}{\max(RMSE_{ecoD})} + \frac{RMSE_{FH_i}}{\max(RMSEP_{FH})} + \frac{RMSEP_{endoD_i}}{\max(RMSEP_{endoD})} +$$

$$9 \quad \frac{RMSEP_{ecoD_i}}{\max(RMSEP_{ecoD})} + \frac{RMSEP_{FH_i}}{\max(RMSEP_{FH})} \quad (6)$$

10 **Results**

11 *Effects of D_{CA} on model accuracy*

12 Fixed D_{CA} only had a relatively small effect on the quality of the fit ($12.3 < RMSE_{endoD} <$
 13 15.1 days; coefficient of variation $CV = 6.8\%$ for a 153 days range) and the predictive ability
 14 of D_{ER} ($8.3 < RMSEP_{endoD} < 11.8$ days; $CV = 11.7\%$). Fixed D_{CA} between DOY 223 (Aug. 11th)
 15 and 274 (Oct. 1st) are relatively efficient to simulate CU accumulation with respect to D_{ER} . The
 16 effect of various D_{CA} on the prediction of D_{BB} was also relatively low for the quality of the fit
 17 ($7.1 < RMSE_{ecoD} < 8.6$ day; $CV = 6.1\%$) and the predictive ability ($6.9 < RMSEP_{ecoD} < 8.1$
 18 days; $CV = 4.7\%$). A wider range of fixed D_{CA} , *i.e.* between 223 and 325 (Nov. 21st), similarly
 19 performed for D_{BB} prediction. Annual phenological cycle (D_{ER} and D_{BB}) was thus best predicted
 20 when D_{CA} was set to DOY 254 (*i.e.* Sep. 11th). For frost hardiness, fixed D_{CA} earlier than DOY
 21 305 (Nov. 1st) provided highly efficient fit ($RMSE < 2.0^\circ C$). However, the prediction was not
 22 accurate enough, as $RMSEP$ was almost twice higher ($3.2 < RMSEP < 3.9^\circ C$).

1 The D_{CA} returned by the various dynamic functions were highly different across France:
2 from DOY 182 ± 5 to 312 ± 14 (median \pm SD; Fig. 1A). Four groups of earliness can be defined:
3 very early (T_{min} and photoperiod), early (DP_E , $LFPT_{mod}$ and LFT_{mod}), intermediate (CU_{min}) and
4 late (LFT_{ori} , $LFPT_{ori}$, DP_{ori} , DP_L and FF). All the dynamic D_{CA} computed via different functions
5 exhibited highly significant correlation with mean annual temperature of the site (Fig. 1B-D).

6 Simple temperature thresholds, such as T_{min} or T_{mean} did not provide accurate phenological
7 (RMSEP > 11.5 and 8.0 days for D_{ER} and D_{BB} , respectively) nor FH prediction (RMSEP $>$
8 3.3°C ; Tab. 2). The D_{CA} calculated via a photoperiodic threshold was relatively efficient to
9 predict D_{BB} (RMSEP = 6.8 days), but not D_{ER} (RMSEP = 10.2 days) nor FH (RMSEP = 3.5°C).

10 The D_{CA} computed using the Utah function did not provide accurate prediction for any
11 variable of interest (RMSEP = 14.1 days, 7.8 days and 3.5°C for D_{ER} , D_{BB} and FH,
12 respectively). The leaf fall thermal function (LFT), using either the original (LFT_{ori}) or the
13 modified sets of parameters (LFT_{mod}), was relatively efficient to predict D_{BB} (RMSEP = 7.23
14 days) but less efficient for D_{ER} and FH (RMSEP ≥ 9.2 and 3.2 for D_{ER} and FH, respectively).
15 The leaf fall photothermal function (LFPT) provided accurate predictions for phenological
16 dates (RMSEP ≤ 8.8 and 6.9 days for D_{ER} and D_{BB} respectively) but not for FH (RMSEP > 3.2
17 $^\circ\text{C}$). The D_{CA} computed using the DORMPHOT function were the most efficient to predict D_{ER} ,
18 D_{BB} and FH, in the original and ‘Late’ versions of the function (DP_{ori} , and DP_L , respectively).
19 Finally, the performance index (PI) accounting for all the models and methods of computing
20 D_{CA} could not distinguish between DP_{ori} and DP_L (PI = 6.31).

21 Finally, the different processes exhibited contrasted thickness linkage with D_{CA} . For
22 ecodormancy, a wide range of fixed date (100 days range: Aug. 11th until Nov. 21st) and all the
23 computations using photoperiod as an input variable, provided good fit and predictive
24 accuracies (RMSE_{EcoD} and RMSE_{EndoD} lower than 8 and 7.6 days, respectively). Endodormancy
25 release was slightly more restrictive with the best predictions either provided by fixed calendar

1 dates (Aug. 11th until Oct. 1st) or dynamic functions integrating the interaction between
2 temperature and photoperiod (LFPT and DP). Frost hardness was the most restrictive, with
3 excellent predictive accuracy when using D_{CA} computed by DORMPHOT model (DP_{ori} and
4 DP_L ; $RMSEP < 3.0^\circ C$) compared to all the other computations.

5 Although both DP_{ori} and DP_L performed almost equally for the three variables of interest
6 (D_{ER} , D_{BB} and FH), DP_L exhibited a slightly better correlation to predict the dynamic of Mean
7 Time until budburst (MTB) during the period of dormancy induction ($R^2 = 0.262$ and 0.282 for
8 DP_{ori} and DP_L , respectively; Fig. 2 A-C). Furthermore, as FH was slightly better predicted using
9 DP_L ($RMSEP = 2.6^\circ C$), D_{CA} predicted by this function was selected to predict the current and
10 future frost risks (Fig. 3).

11 *Predictions under current and future climates for Juglans regia cv Franquette*

12 Using D_{CA} computed from DP_L endodormancy release dates under current climate exhibited
13 a structured geographical pattern across France. Endodormancy release dates spanned over a
14 60 days range (Fig. 3A): earlier in mountain area (Early December) and later on the
15 Mediterranean (South-East Mid-February) and southwestern coasts (Late January). Budburst
16 dates exhibited an opposite pattern over a 77 days range (Fig. 3B): from Mid-April in Southern
17 and Western parts until late June in mountainous area. Endodormancy release and budburst
18 dates were highly correlated to mean annual temperature, although through different functions
19 (exponential and cubic function for endodormancy release and budburst, respectively; Fig. 3C-
20 D).

21 The geographic structure was less obvious for frost damages, with very low predicted
22 damages during autumn (Fig. 4A) and spring (Fig. 4C), except in high mountain area. During
23 the winter period, higher frost damages are predicted in the northeastern part of France
24 (Burgundy, Alsace, Lorraine), in mountain areas and in the north of Rhone valley (Fig. 4B).
25 Average predicted damages in autumn and spring were highly correlated to the date of first (<-

1 4°C) and last frost event ($< 0^{\circ}\text{C}$), respectively (Fig. 4D; F), whereas maximum winter damages
2 were correlated to absolute annual temperature (Fig. 4E).

3 For *J. regia* cv Franquette, similar trends are observed under future climate predictions, with
4 high delay in both the onset of dormancy and release for mean annual temperature higher than
5 5°C (Fig. 5A, B). However, the delay affecting endodormancy stage does not carry over toward
6 budburst with earlier budburst with increasing temperature for lower mean annual temperature
7 than 10°C (Fig. 5C). It should be noted that similar or earlier budburst is likely to happen for
8 higher temperature, and this may be observed in up to one quarter of France at the end of the
9 XXIst century: from 5 (RCP 4.5) to 27% (RCP8.5 scenario) of the French territory in 2051-2100
10 (Fig. 6). The results are geographically consistent with the use of a fixed D_{CA} , but through a
11 wider range in 2051-2100 (Fig. S3). Although such a delay is not forecasted within the ‘Noix
12 de Grenoble’ Protected Designation of Origin area (Middle East), budburst would be delayed
13 in most of the ‘Noix du Périgord’ area (Middle West) under RCP8.5 scenario (75.1% 2006-
14 2050 and 94.2% 2051-2100). Overall, frost damages are expected to decrease, on average, all
15 over France (Fig. S1). However, in North East and Massif Central, higher decennial risks are
16 predicted under RCP 2.6 *scenario* (2006-2051; Fig. S2).

17 **Discussion**

18 Defining the initial date for cyclical processes is a critical issue. To predict annual
19 phenological cycle in perennial organisms, such as trees, various empirical rules have been used
20 so far. The onset of chilling accumulation during endodormancy stage (D_{CA}) had, for instance,
21 been arbitrarily set using fixed dates across years and locations (Chuine *et al.*, 2016) or, under
22 the dependence of environmental factors controlling the induction of dormancy (Caffarra *et al.*,
23 2011b). In the current study, long-term observations of phenological stages (endodormancy
24 release and budburst) and related processes (frost acclimation and deacclimation) were used in

1 various environmental conditions and showed that the DORMPHOT model was the most
2 relevant to predict winter biology in walnut trees.

3 Depending on the studied process, not all computation performed equally (Tab. 2). The
4 effect of D_{CA} on ecodormancy and budburst was buffered during endodormancy release. From
5 a budburst perspective, various rules for D_{CA} computation can thus be considered as valid,
6 although they all consider a potential effect of photoperiod, either directly or indirectly via fixed
7 date (Welling *et al.*, 1997; Chuine and Régnière, 2017). A narrower range of fixed date and
8 fewer dynamic computations of D_{CA} (DORMPHOT and LFPT models) provided accurate
9 predictions for endodormancy release dates. However, providing predictive rules only based on
10 one or two phenological stages, even though with a large number of measurements (more than
11 100 dates, combining endodormancy and budburst, in the present study) does not provide
12 sufficient details for continuous process modeling. Introducing frost hardiness as a co-variable
13 of dormancy induction and release provided higher temporal resolution into these concurring
14 processes (Welling & Palva, 2006; Charrier *et al.*, 2011; Hanninen, 2016). Through a multi
15 criterion analysis, the D_{CA} simulated by the DORMPHOT model provided the most accurate
16 predictions. This model, originally developed in *Betula pubescens*, is thus relevant for other
17 deciduous species such as *Juglans regia*. The conceptual development of this model is indeed
18 based on experimental results combining photoperiod and temperature manipulation (Caffarra
19 *et al.*, 2011b), whereas other formalisms were based on empirical observations (*e.g.* leaf fall).
20 Photoperiod and temperature are intimately related in controlling annual weather dynamics.
21 However, temperature fluctuation is much higher at a given date of the year which could induce
22 high variability in the onset of the winter season (see *e.g.* Fig.1). Since dormancy induction and
23 frost acclimation are lengthy processes (*e.g.* ca. 1-2 month), perennial plants cannot only rely
24 on temperature changes that can be too sudden for the onset of winter rest (Caffarra *et al.*,
25 2011a). Both photoperiod and temperature variables thus affect annual phenological cycle in

1 perennial plants, although at different ratio across species. Photoperiod is for instance
2 predominant in *Populus* (Kalcsits *et al.*, 2009) and *Vitis* (Fennel & Hoover, 1991), while
3 temperature in *Malus* and *Pyrus* (Heide & Prestrud, 2005) and *Sorbus* (Heide, 2011). The
4 interaction of both photoperiod and temperature has been showed in *Prunus* (Heide, 2008).
5 Integrating both variables is an interesting strategy to prevent dormancy induction during cold
6 late summer (without frost risks) while maintaining physiological activity under extended warm
7 periods. It has been hypothesized that the modulation of photoperiod sensitivity by temperature
8 may be related by thermal effect on phytochrome perception of day length (Mølmann *et al.*,
9 2005).

10 The selected rule for D_{CA} , predicting a delayed chilling accumulation in warmer locations
11 ($> 7^{\circ}\text{C}$ MAT; Fig. 1C; 5A) would further delay endodormancy release in such area (Fig. 3 A,
12 C). However, cold weather would limit ontogenetic development during ecodormancy,
13 providing a negative picture of D_{ER} vs D_{BB} (Fig. 3). Under future climatic conditions such as
14 predicted by RCPs *scenarii*, this picture is likely to be blurred as the tipping point for budburst
15 of *J. regia* cv Franquette would be achieved (*ca.* 14°C MAT). Below 14°C , endodormancy
16 would be released and warmer temperature of the winter-spring period lead to earlier budburst.

17 Date of first frost ($< 0^{\circ}\text{C}$), minimum temperature and date of late frost ($< -4^{\circ}\text{C}$) appear as
18 good proxies to predict early, maximum and late frost damages, respectively (Fig. 4D-F).
19 Predicted minimal temperature are expected to decrease as well and, even though flushing buds
20 would be highly vulnerable to late frost, they are likely not to be exposed to damaging
21 temperature (Fig. 4). Although climate models agree on the average trend, they are still unclear
22 on the climate extreme events such as early and late frost events. Notably, the decennial
23 damages (*i.e.* maximum damage occurring every ten years) may increase in North East and
24 Massif Central area (Fig. S2). The relative balance between photo- and thermosensitivity is
25 likely to be a critical trait explaining this trend. In the near future in these areas, minimum

1 temperature are still likely to happen while dormancy induction and frost acclimation would be
2 delayed by mean temperature increase.

3 Above the 14°C threshold, endodormancy induction and release would be more delayed than
4 ecodormancy hastened, resulting in delayed budburst due to a lack of chilling, compared to the
5 present situation. This situation would cover up to one quarter of France under RCP 8.5 scenario
6 (Fig. 6). Although it would significantly reduce frost damages, even under false spring *scenarii*,
7 lack of chilling would induce severe agronomic troubles such as erratic patterns of blooming,
8 floribondity, and potential dischronism with anthesis. A similar pattern is also expected using
9 fixed date (see Fig S3).

10 With respect to French nuts production, both IGP regions would face distinct threats as they
11 stand on both sides of the 14°C MAT tipping point. In the Périgord, chilling requirements are
12 likely not to be met and lower chilling varieties have to be selected, as the current ones do not
13 exhibit variability for this trait (Charrier *et al.*, 2011). In Grenoble, earlier budburst dates are
14 expected, leading to higher exposure to frost events, and varieties with higher forcing
15 requirements may help to stabilize the production (Charrier *et al.*, 2018). However, both regions
16 seem relatively safe with respect to frost damages.

17 **Conclusions and perspectives**

18 This study highlighted the relevance of dynamic dates for simulating annual phenological
19 cycle and frost acclimation. The DORMPHOT model, integrating temperature and
20 photoperiodic control of dormancy induction, is the most efficient for all studied processes. On
21 one hand, higher decennial damages would be observed in the near future on *ca.* 15% of French
22 territory because of late frost acclimation. On the other hand, the tipping point for phenological
23 processes is likely to be reached during the XXIst century with chilling requirements that are

- 1 likely not to be fulfilled. The correlation between MAT, phenological stages and frost damages
- 2 is an important tool, to build relevant meta-models at the global scale.

3

1 REFERENCES

- 2 Arora, R., Rowland, L. J., & Tanino, K. (2003). Induction and release of bud dormancy in
3 woody perennials: a science comes of age. *HortScience*, 38(5), 911-921.
- 4 Balandier, P., Gendraud, M., Rageau, R., Bonhomme, M., Richard, J. P., & Parisot, E. (1993).
5 Bud break delay on single node cuttings and bud capacity for nucleotide accumulation as
6 parameters for endo-and paradormancy in peach trees in a tropical climate. *Scientia*
7 *Horticulturae*, 55(3-4), 249-261.
- 8 Basler, D., & Körner, C. (2012). Photoperiod sensitivity of bud burst in 14 temperate forest tree
9 species. *Agricultural and Forest Meteorology*, 165, 73-81.
- 10 Caffarra, A., Donnelly, A., Chuine, I., & Jones, M. B. (2011a). Modelling the timing of *Betula*
11 *pubescens* budburst. I. Temperature and photoperiod: a conceptual model. *Climate*
12 *Research*, 46(2), 147-157.
- 13 Caffarra, A., Donnelly, A., & Chuine, I. (2011b). Modelling the timing of *Betula pubescens*
14 budburst. II. Integrating complex effects of photoperiod into process-based models. *Climate*
15 *research*, 46(2), 159-170.
- 16 Charrier, G., & Améglio, T. (2011). The timing of leaf fall affects cold acclimation by
17 interactions with air temperature through water and carbohydrate contents. *Environmental*
18 *and Experimental Botany*, 72(3), 351-357.
- 19 Charrier, G., Bonhomme, M., Lacoite, A., & Améglio, T. (2011). Are budburst dates,
20 dormancy and cold acclimation in walnut trees (*Juglans regia* L.) under mainly genotypic or
21 environmental control?. *International journal of biometeorology*, 55(6), 763-774.
- 22 Charrier, G., Chuine, I., Bonhomme, M., & Améglio, T. (2018). Assessing frost damages using
23 dynamic models in walnut trees: exposure rather than vulnerability controls frost risks.
24 *Plant, Cell & Environment*, 41(5), 1008-1021.
- 25 Chuine, I., & Régnière, J. (2017). Process-based models of phenology for plants and animals.
26 *Annual Review of Ecology, Evolution, and Systematics*, 48, 159-182.
- 27 Chuine, I., Bonhomme, M., Legave, J. M., García de Cortázar-Atauri, I., Charrier, G., Lacoite,
28 A., & Améglio, T. (2016). Can phenological models predict tree phenology accurately in the
29 future? The unrevealed hurdle of endodormancy break. *Global Change Biology*, 22(10),
30 3444-3460.
- 31 Delpierre, N., Dufrière, E., Soudani, K., Ulrich, E., Cecchini, S., Boé, J., & François, C. (2009).
32 Modelling interannual and spatial variability of leaf senescence for three deciduous tree
33 species in France. *Agricultural and Forest Meteorology*, 149(6-7), 938-948.
- 34 Dennis, F. G. (2003). Problems in standardizing methods for evaluating the chilling
35 requirements for the breaking of dormancy in buds of woody plants. *HortScience*, 38(3),
36 347-350.
- 37 Déqué, M., Rowell, D. P., Lüthi, D., Giorgi, F., Christensen, J. H., Rockel, B., ... & van den
38 Hurk, B. J. J. M. (2007). An intercomparison of regional climate simulations for Europe:
39 assessing uncertainties in model projections. *Climatic Change*, 81(1), 53-70.
- 40 Fennell, A., & Hoover, E. (1991). Photoperiod influences growth, bud dormancy, and cold
41 acclimation in *Vitis labruscana* and *V. riparia*. *Journal of the American Society for*
42 *Horticultural Science*, 116(2), 270-273.
- 43 Ferguson, J. C., Tarara, J. M., Mills, L. J., Grove, G. G., & Keller, M. (2011). Dynamic thermal
44 time model of cold hardiness for dormant grapevine buds. *Annals of botany*, 107(3), 389-
45 396.
- 46 Gauzere, J., Lucas, C., Ronce, O., Davi, H., & Chuine, I. (2019). Sensitivity analysis of tree
47 phenology models reveals increasing sensitivity of their predictions to winter chilling
48 temperature and photoperiod with warming climate. *Ecological Modelling*, 411, 108805.

- 1 Hänninen, H., & Tanino, K. (2011). Tree seasonality in a warming climate. *Trends in plant*
2 *science*, 16(8), 412-416.
- 3 Hänninen, H. (2016). Boreal and temperate trees in a changing climate. *Dordrecht: Springer*.
4 *doi*, 10, 978-94.
- 5 Heide, O. M., & Prestrud, A. K. (2005). Low temperature, but not photoperiod, controls growth
6 cessation and dormancy induction and release in apple and pear. *Tree physiology*, 25(1),
7 109-114.
- 8 Heide, O. M. (2008). Interaction of photoperiod and temperature in the control of growth and
9 dormancy of *Prunus* species. *Scientia Horticulturae*, 115(3), 309-314.
- 10 Heide, O. M. (2011). Temperature rather than photoperiod controls growth cessation and
11 dormancy in *Sorbus* species. *Journal of experimental botany*, 62(15), 5397-5404.
- 12 Kalcsits, L. A., Silim, S., & Tanino, K. (2009). Warm temperature accelerates short
13 photoperiod-induced growth cessation and dormancy induction in hybrid poplar (*Populus*×
14 *spp.*). *Trees*, 23(5), 971-979.
- 15 Landsberg, J. J. (1974). Apple fruit bud development and growth; analysis and an empirical
16 model. *Annals of Botany*, 38(5), 1013-1023.
- 17 Lang, G. A., Early, J. D., Martin, G. C., & Darnell, R. L. (1987). Endo-, para-, and
18 ecodormancy: physiological terminology and classification for dormancy research.
19 *HortScience*, 22(3), 371-377.
- 20 Leinonen, I. (1996). A simulation model for the annual frost hardiness and freeze damage of
21 Scots pine. *Annals of Botany*, 78(6), 687-693.
- 22 Luedeling, E. (2019) Statistical Methods for Phenology Analysis in Temperate Fruit Trees,
23 chillR Package.
- 24 Mauget, J. C., (1980). Dormance et précocité de débourrement des bourgeons chez quelques
25 cultivars de Noyer (*Juglans regia* L.).
- 26 Maurya, J. P., & Bhalerao, R. P. (2017). Photoperiod-and temperature-mediated control of
27 growth cessation and dormancy in trees: a molecular perspective. *Annals of botany*, 120(3),
28 351-360.
- 29 Meier, U. (2001). Growth stages of mono- and dicotyledonous plants. BBCH Monograph. doi:
30 10.5073/bbch0515.
- 31 Mølmann, J. A., Asante, D. K., Jensen, J. B., Krane, M. N., Ernstsens, A., Junttila, O., & Olsen,
32 J. E. (2005). Low night temperature and inhibition of gibberellin biosynthesis override
33 phytochrome action and induce bud set and cold acclimation, but not dormancy in PHYA
34 overexpressors and wild-type of hybrid aspen. *Plant, Cell & Environment*, 28(12), 1579-
35 1588.
- 36 Rageau, R. (1982). Etude expérimentale des lois d'action de la température sur la croissance
37 des bourgeons floraux du pêcher (*Prunus persica* L. Batsch) pendant la postdormance.
- 38 Réaumur, R. A. F. d. 1735. Observations du thermomètre, faites à Paris durant l'année 1735,
39 comparées avec celles qui ont été faites sous la ligne, à l'isle de France, à Alger et quelques
40 unes de nos isles de l'Amérique. Mémoires de l'Académie des Sciences de Paris.
- 41 Repo, T., & Lappi, J. (1989). Estimation of standard error of impedance-estimated frost
42 resistance. *Scandinavian Journal of Forest Research*, 4(1-4), 67-74.
- 43 Richardson, E. A., EA, R., SD, S., & DR, W. (1974). A model for estimating the completion of
44 rest for "Redhaven" and "Elberta" peach trees.
- 45 Vegis, A. (1964). Dormancy in higher plants. *Annual review of plant physiology*, 15(1), 185-
46 224.
- 47 Weinberger, J. H. (1950). Chilling requirements of peach varieties. In *Proceedings. American*
48 *Society for Horticultural Science* (Vol. 56, pp. 122-8).

- 1 Weinberger, J. H. (1956). Prolonged dormancy trouble in peaches in the southeast in relation
2 to winter temperatures. *Journal of the American Society for Horticultural Science*, 67, 107-
3 112.
- 4 Weinberger, J. H. (1967). Some temperature relations in natural breaking of the rest of Peach
5 flower buds in the San Joaquin Valley, California. *Proceedings of the American Society for*
6 *Horticultural Science*, 51, 84-89.
- 7 Welling, A., & Palva, E. T. (2006). Molecular control of cold acclimation in trees. *Physiologia*
8 *Plantarum*, 127(2), 167-181.
- 9 Welling, A., Kaikuranta, P., & Rinne, P. (1997). Photoperiodic induction of dormancy and
10 freezing tolerance in *Betula pubescens*. Involvement of ABA and dehydrins. *Physiologia*
11 *Plantarum*, 100(1), 119-125.
- 12 Welling, A., Moritz, T., Palva, E. T., & Junttila, O. (2002). Independent activation of cold
13 acclimation by low temperature and short photoperiod in hybrid aspen. *Plant Physiology*,
14 129(4), 1633-1641.
- 15 Zhang, M. I. N., & Willison, J. H. M. (1987). An improved conductivity method for the
16 measurement of frost hardiness. *Canadian Journal of Botany*, 65, 710–715.
- 17

1 **Acknowledgements**

2 The author wants to acknowledge the essential contribution of Marc Bonhomme, Aline Faure,
3 Jean-Claude Mauget, Remi Rageau, Jean-Pierre Richard for dormancy release date
4 measurements. Phenological data and stem materials were provided by Neus Aleita, Romain
5 Baffoin, Fabrice Lheureux, Marianne Naudin and Eloise Tranchand. The author is also thankful
6 to Thierry Améglio, André Lacointe and Heikki Hanninen for constructive comments on
7 preliminary versions of the manuscript. Part of the collected data were supported by the Pôle
8 National de Données de la Biodiversité (a.k.a SOERE Tempo).
9

1 **Figure captions**

2 **Figure 1. A** Distribution of date at the onset of chilling accumulation T_0 across France
3 over the 1950-2005 period according to different computations: T_{min} minimum
4 temperature (lower than 15.28°C), DP DORMPHOT model from different sets of
5 parameters (O: original, E early, L Late), LFT_{mod} Leaf Fall model (thermal version
6 modified), LFPT Leaf Fall model Photothermal version Original and modified. B, C and
7 D T_0 depending on mean annual temperature.

8 **Figure 2** Mean time until budbreak at 25°C (MTB) depending on the day after
9 September 1st (A), Dormancy stage computed according to the DORMPHOT model
10 (B original version, C, late version).

11 **Figure 3. A-B.** Average dates of endodormancy release (A) and budburst (B)
12 predicted across France under current climatic conditions. **C-D.** Average dates of
13 endodormancy release (C) and budburst (D) depending on mean annual temperature
14 (°C) across France.

15 **Figure 4. A-C.** Average frost damages predicted across France under current
16 climatic conditions in autumn (A), winter (B) and spring (C). **D.** Average early frost
17 damages depending on the average date of the first frost lower than 0°C. **E.** Average
18 maximum frost damages depending on the average annual minimum temperature. **F.**
19 Average late frost damages depending on the average date of the last frost lower
20 than -4°C.

21 **Figure 5. A-C.** Average date of onset of dormancy (A), endodormancy release (B),
22 budburst (C) over France depending on the mean annual temperature under current
23 climate (gray), RCP 2.6 (2006-2051 cyan, 2051-2100 blue), RCP 4.5 (2006-2051
24 green, 2051-2100 yellow), and RCP 8.5 *scenarii* (2006-2051 purple, 2051-2100 red).
25 **D.** Average predicted autumn early frost damages depending on the date of first frost
26 (<0°C) **E.** Average predicted maximum winter frost damages depending on the mean
27 absolute minimum temperature **F.** Average predicted spring late frost damages
28 depending on the date of last frost (<-4°C). Each dot represent the average of the
29 considered period at 8 x 8km spatial resolution, black line represent the best non-
30 linear regression.

31 **Figure 6.** Relative change in predicted average budburst date across France
32 according to different climatic *scenarii* and time periods (earlier and later budburst
33 dates than the mean are represented in blue and red, respectively).

34

1 **Table 1. Site and dataset description**

Location	Elevation (m asl.)	Latitude °	Longitude °	Mean annual temperature (°C)	Minimum temperature (°C)	Absolute minimum temperature (°C)	Number of freezing events	First Frost (Autumn) DOY	Last Frost (Spring) DOY	Number of observations (years and number of dates in brackets)					
										Endodormancy Release		Budburst		Frost Hardiness	
										Calibration	Validation	Calibration	Validation	Calibration	Validation
Balandran	69	43.758	4.516	16.90	12.00	-3.78	14.5	340	50	1	1	0	0	0	0
Chatte	304	45.143	5.282	13.62	8.15	-9.39	61.7	308	102	0	0	12	11	0	1 (6)
Creyse	115	44.887	1.597	14.65	8.52	-8.50	52.4	309	104	0	0	13	12	0	1 (8)
Crouël	340	45.779	3.142	13.25	9.26	-11.51	59.6	302	108	13	12	4	4	5 (49)	2 (21)
Orcival	1150	45.683	2.842	12.92	7.72	-12.13	97.4	291	126	1	1	1	0	0	0
Terrasson	90	45.136	1.300	14.61	8.96	-9.69	47.4	311	100	1	1	1	0	0	0
Theix	945	45.706	3.021	9.70	6.22	-15.11	100.3	282	129	1	1	1	0	1 (11)	1 (9)
Toulenne	22	44.557	-0.263	15.38	10.56	-6.09	25.9	325	74	1	0	9	9	0	0
Mas Bové	112	41.170	1.169	15.87	10.81	-4.05	14.9	343	47	0	0	0	0	0	1 (7)

2

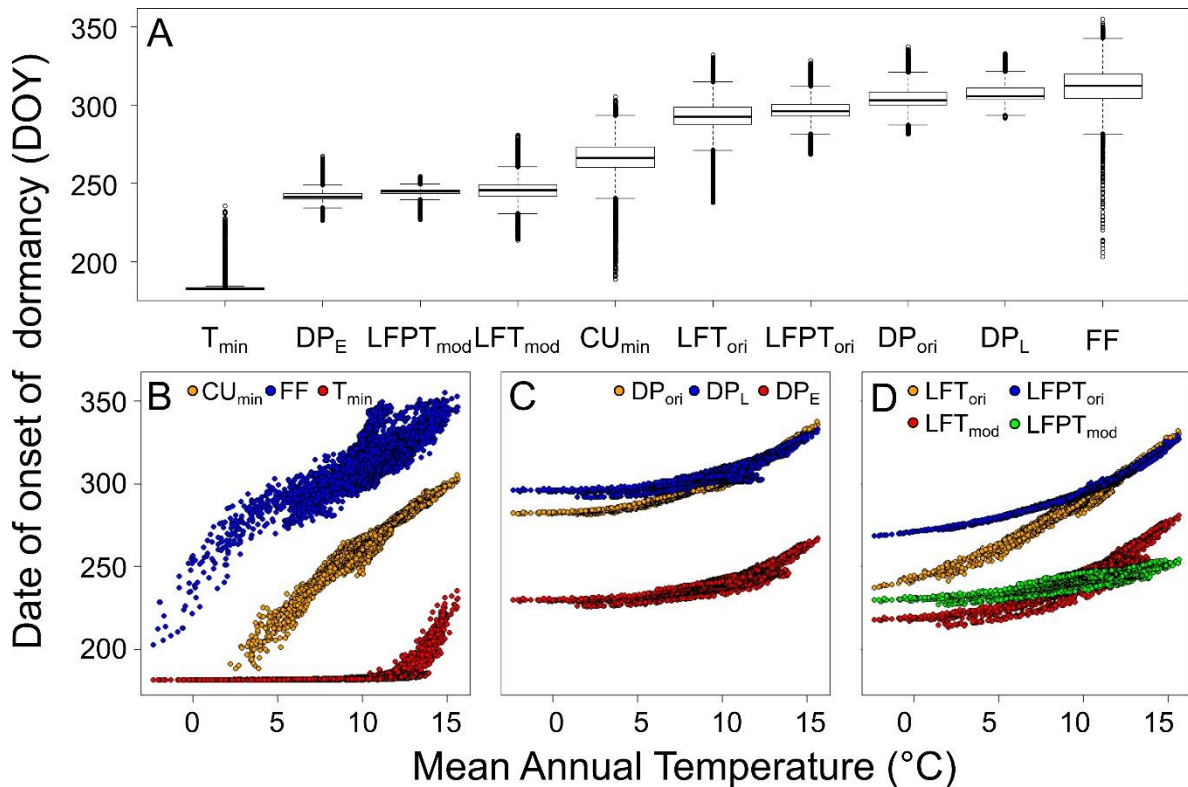
3

1 **Table 2.** Quality assessment of different models. RMSE(P) less than 15% higher than minimum RMSE or RMSEP are indicated in bold. Dates for
2 onset of chilling accumulation (D_{CA}) were either fixed or computed according to date of first frost (FF), minimum temperature (T_{min}), mean
3 temperature (T_{mean}), photoperiod, minimum chilling unit (CU_{min}), Leaf fall using temperature (LFT) and temperature and photoperiod (LFPT) and
4 dormphot (DP). Ori and mod refer to the original published version (ori) or modified for walnut (mod), E and L for Early and Late.

			Endodormancy	Budburst	Frost	PI			
Type	Function	D_{CA}	Release Date		Date		Hardiness		
			RMSE (days)	RMSEP (days)	RMSE (days)	RMSEP (days)	RMSE (°C)	RMSEP (°C)	
Fixed		182 (Jul. 1 st)	12.84	11.84	8.58	8.08	1.79	3.52	7.31
		192 (Jul. 11 th)	12.64	11.48	8.44	7.57	1.79	3.39	7.10
		202 (Jul.21 st)	12.41	10.73	8.25	7.28	1.80	3.42	6.94
		213 (Aug. 1 st)	12.33	10.06	8.06	7.14	1.79	3.46	6.81
		223 (Aug. 11 th)	12.65	9.36	7.78	6.89	1.78	3.49	6.68
		233 (Aug. 21 st)	12.68	8.71	7.61	6.85	1.78	3.49	6.58
		244 (Sep. 1 st)	12.87	8.75	7.39	7.03	1.79	3.48	6.59
		254 (Sep. 11 th)	13.19	8.49	7.26	6.88	1.77	3.47	6.53
		264 (Sep. 21 st)	13.70	8.80	7.15	7.24	1.74	3.24	6.55
		274 (Oct. 1 st)	13.80	8.47	7.25	7.38	1.73	3.29	6.56
		284 (Oct. 11 th)	13.98	8.29	7.10	6.93	1.77	3.37	6.52
		294 (Oct. 21 st)	14.39	8.47	7.25	7.15	1.84	3.30	6.64
		305 (Nov. 1 st)	14.48	9.22	7.45	7.47	1.84	3.21	6.78
		315 (Nov. 11 th)	14.48	9.93	7.52	7.56	2.15	3.42	7.16
		325 (Nov. 21 st)	14.67	10.26	7.46	7.43	2.90	3.90	7.81
	335 (Dec. 1 st)	15.10	10.33	7.58	7.67	3.77	3.52	8.77	
Dynamic	Simple	FF	17.71	14.15	9.35	15.69	1.90	4.92	9.84
		T_{min}	12.88	11.93	8.55	8.03	1.79	3.37	7.25
		T_{mean}	12.93	11.59	8.70	8.47	1.81	3.38	7.31
		Photoperiod	12.31	10.24	7.94	6.85	1.80	3.46	6.78
	Complex	CU_{min}	16.32	14.08	8.22	7.78	1.78	3.48	7.74
		LFT _{ori}	12.91	10.37	8.11	7.23	1.76	3.22	6.81
		LFT _{mod}	12.57	9.16	8.11	7.23	1.80	3.19	6.83
		LFPT _{ori}	13.34	8.67	7.42	6.72	1.83	3.24	6.51
		LFPT _{mod}	12.66	8.81	7.43	6.89	1.78	3.50	6.57
		DP _{ori}	13.01	8.81	7.47	6.61	1.76	2.87	6.31
		DP _E	12.05	8.64	7.73	7.24	1.80	3.95	6.77
DP _L	12.51	9.43	7.52	7.14	1.70	2.65	6.31		

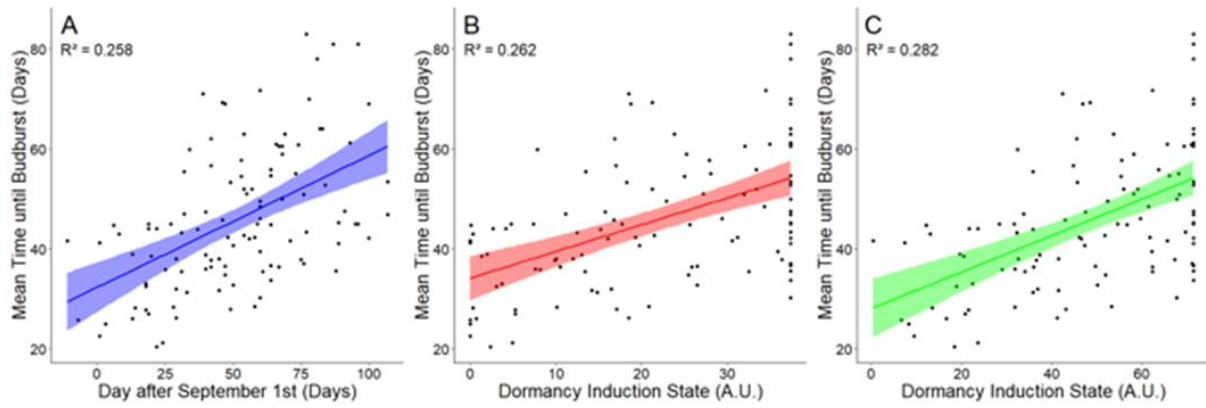
5

1 **Figure captions**



2
3 **Figure 1.** A Distribution of date at the onset of chilling accumulation T_0 across France
4 over the 1950-2005 period according to different computations: T_{min} minimum
5 temperature (lower than 15.28°C), DP DORMPHOT model from different sets of
6 parameters (O: original, E early, L Late), LFT_{mod} Leaf Fall model (thermal version
7 modified), LFPT Leaf Fall model Photothermal version Original and modified. B, C and
8 D T_0 depending on mean annual temperature.

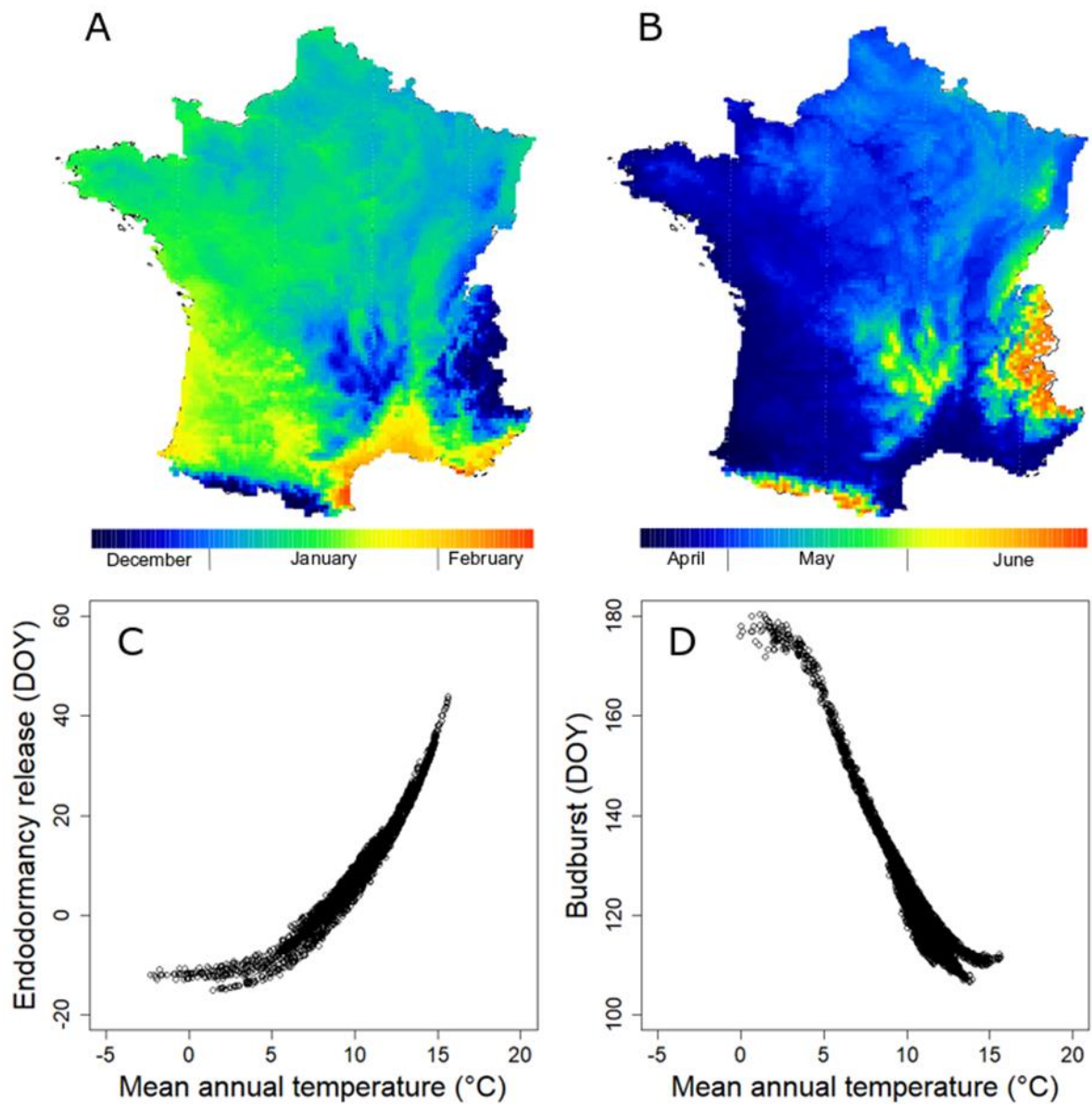
9



1

2 **Figure 2** Mean time until budbreak at 25°C (MTB) depending on the day after
 3 September 1st (A), Dormancy stage computed according to the DORMPHOT model
 4 (B original version, C, late version).

5

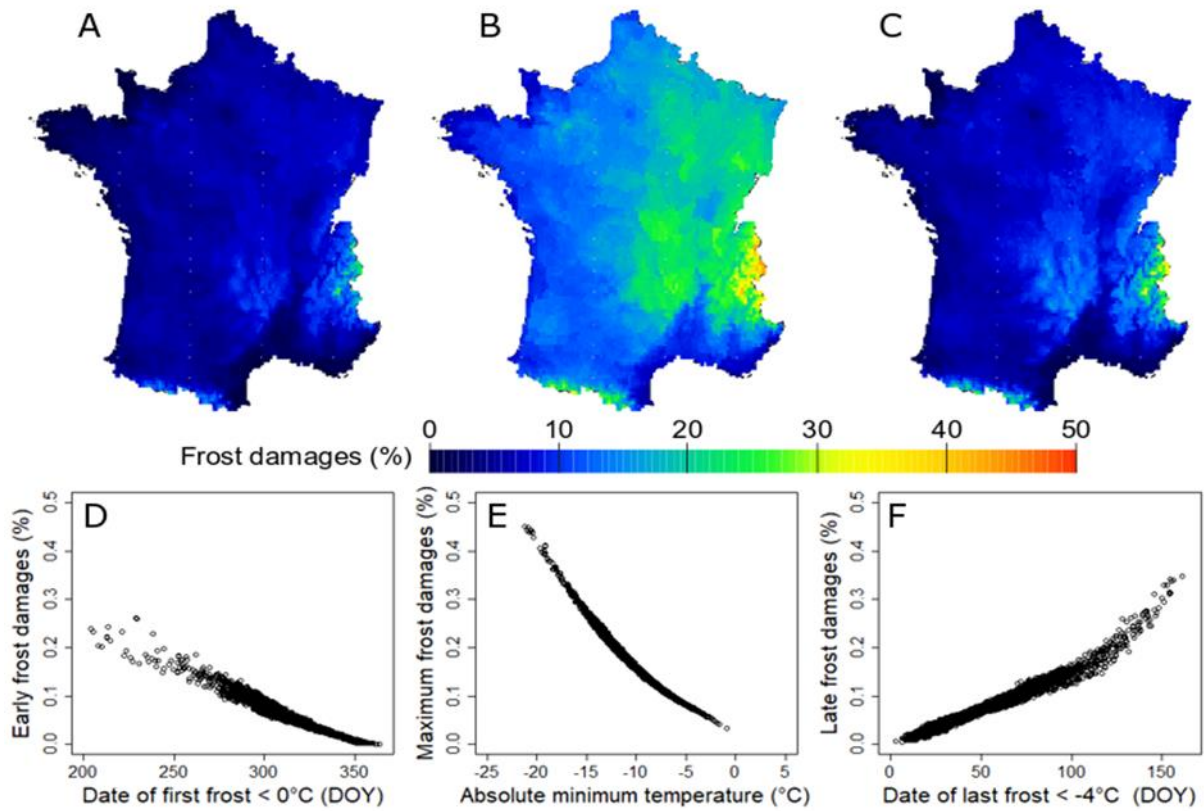


1

2 **Figure 3. A-B.** Average dates of endodormancy release (A) and budburst (B)
 3 predicted across France under current climatic conditions. **C-D.** Average dates of
 4 endodormancy release (C) and budburst (D) depending on mean annual temperature
 5 (°C) across France.

6

1



2

3

4

5

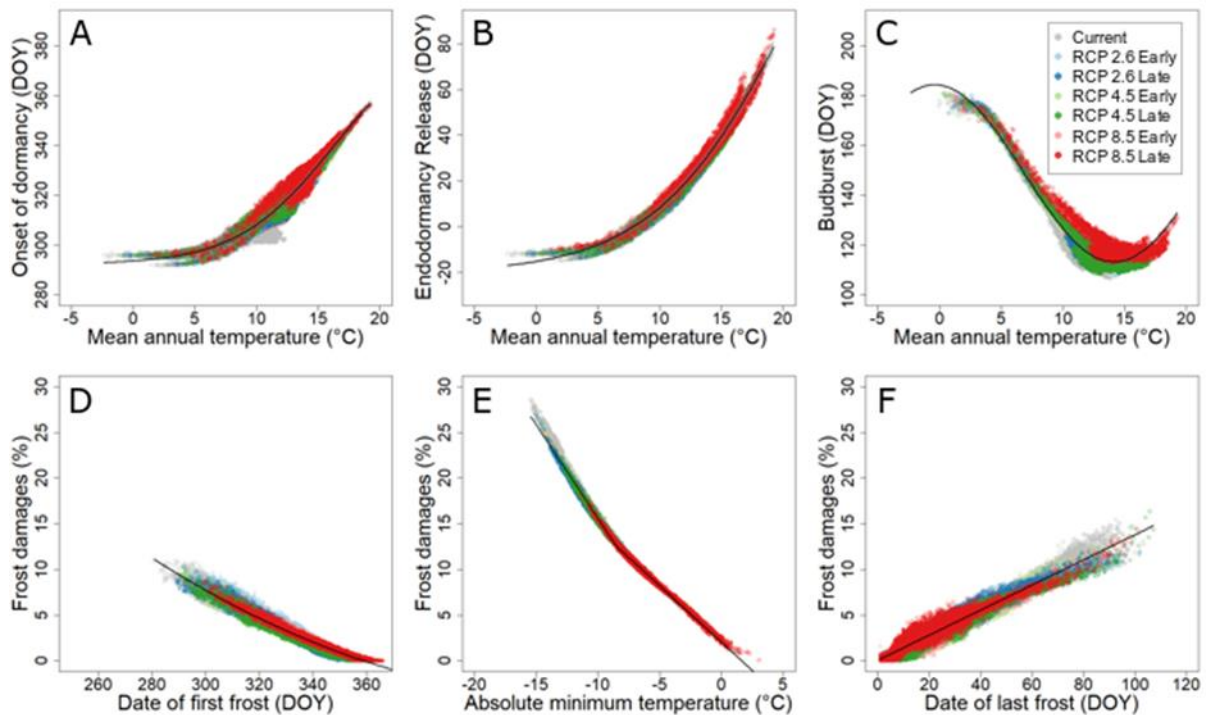
6

7

8

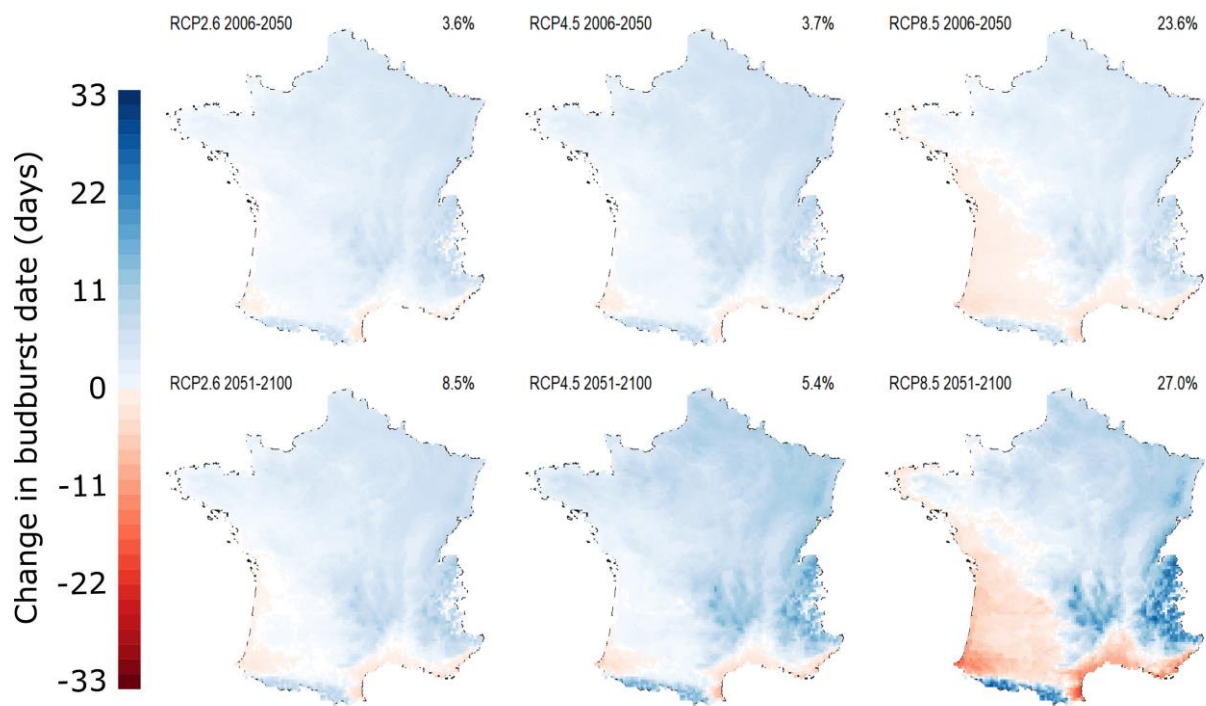
9

Figure 4. A-C. Average frost damages predicted across France under current climatic conditions in autumn (A), winter (B) and spring (C). D. Average early frost damages depending on the average date of the first frost lower than 0°C. E. Average maximum frost damages depending on the average annual minimum temperature. F. Average late frost damages depending on the average date of the last frost lower than -4°C.



1
 2 **Figure 5. A-C.** Average date of onset of dormancy (A), endodormancy release (B),
 3 budburst (C) over France depending on the mean annual temperature under current
 4 climate (gray), RCP 2.6 (2006-2051 cyan, 2051-2100 blue), RCP 4.5 (2006-2051
 5 green, 2051-2100 yellow), and RCP 8.5 *scenarii* (2006-2051 purple, 2051-2100 red).
 6 **D.** Average predicted autumn early frost damages depending on the date of first frost
 7 (<0°C) **E.** Average predicted maximum winter frost damages depending on the mean
 8 absolute minimum temperature **F.** Average predicted spring late frost damages
 9 depending on the date of last frost (<-4°C). Each dot represent the average of the
 10 considered period at 8 x 8km spatial resolution, black line represent the best non-
 11 linear regression.

12



1
 2 **Figure 6.** Relative change in predicted average budburst date across France
 3 according to different climatic *scenarii* and time periods (earlier and later budburst
 4 dates than the mean are represented in blue and red, respectively).

1 **Supplementary material figure captions**

2 **Table S1.** Examples of fixed or dynamic date of onset of chilling accumulation (DCA) across
3 various studies aiming at modeling phenology in various species and location. Chilling models
4 are sigmoid (Hanninen, 1990), normal (Chuine, 2000; Chuine et al., 2003), Utah (Richardson
5 et al., 1974) and variations (smoothed Utah: Bonhomme et al., 2010, Positive Utah and positive
6 Chill Unit for low chilling varieties: Gilreath and Buchanan, 1981), Dynamic (Fishman et al.,
7 1987a,b), Chilling Hours (Weinberger; 1967), Bidabé (Bidabé, 1965a, b), Growing Degree Day
8 (Ritchie and NeSmith, 1991). NH and SH mean northern and southern hemisphere,
9 respectively.

10 **Table S2** Optimized parameters for different DCA computations in *Juglans regia* cv Franquette

11 **Figure S1.** Relative change in predicted average frost damages across France according to
12 different climatic *scenarii* (RCP 2.6, RCP 4.5, RCP 8.5), seasons (Early SON, Midwinter DJF
13 and late risks MAM) and time periods (2006-2050 and 2051-2100). Lower and higher damages
14 than the current mean are represented in in red and blue, respectively).

15 **Figure S2.** Relative change in predicted decennial frost damages across France according to
16 different climatic *scenarii* (RCP 2.6, RCP 4.5, RCP 8.5), seasons (Early SON, Midwinter DJF
17 and late risks MAM) and time periods (2006-2050 and 2051-2100). Lower and higher damages
18 than the current 90th percentile are represented in in red and blue, respectively).

19 **Figure S3.** Relative change in predicted budburst date across France according to different
20 climatic *scenarii* (RCP 2.6, RCP 4.5, RCP 8.5), time periods (2006-2050 and 2051-2100) and
21 D_{CA} (September 1st vs DORMPHOT computation) Later and earlier budburst than currently are
22 represented in in red and blue, respectively. The proportion of area showing delayed budburst
23 is indicated for each map.
24